# Hydroxymethyl Group Conformation in Saccharides: Structural Dependencies of $^2J_{HH}$, $^3J_{HH}$, and $^1J_{CH}$ Spin−Spin Coupling Constants

Roland Stenutz,[†] Ian Carmichael,[‡] Göran Widmalm,[§] and Anthony S. Serianni*,[||]

*Department of Chemistry, Swedish University of Agricultural Sciences, P.O. Box 7015, SE-750 07 Uppsala, Sweden, Radiation Laboratory and Department of Chemistry and Biochemistry, University of Notre Dame, Indiana 46556, and Department of Organic Chemistry, Stockholm University, SE-106 91 Stockholm, Sweden*

*serianni.1@nd.edu*

*Received October 9, 2001*

Experimental and theoretical methods have been used to correlate $^2J_{HH}$ and $^3J_{HH}$ values within the exocyclic hydroxymethyl groups ($CH_2OH$) of saccharides with specific molecular parameters, and new equations are proposed to assist in the structural interpretation of these couplings. $^3J_{HH}$ depends mainly on the C−C torsion angle ($\omega$) as expected, and new Karplus equations derived from *J*-couplings computed from density functional theory (DFT) in a model aldopyranosyl ring are in excellent agreement with experimental values and with couplings predicted from a previously reported general Karplus equation. These results confirm the reliability of DFT-calculated $^1H-^1H$ couplings in saccharides. $^2J_{HH}$ values depend on both the C−C ($\omega$) and C−O ($\theta$) torsions. Knowledge of the former, which may be derived from other parameters (e.g., $^3J_{HH}$), allows $\theta$ to be evaluated indirectly from $^2J_{HH}$. This latter approach complements more direct determinations of $\theta$ from $^3J_{HCOH}$ and potentially extends these more conventional analyses to O-substituted systems lacking the hydroxyl proton. $^1J_{CH}$ values within hydroxymethyl fragments were also examined and found to depend on $r_{CH}$, which is modulated by specific bond orientation and stereoelectronic factors. These latter factors could be largely, but not completely, accounted for by C−C and C−O torsional variables, leading to only semiquantitative treatments of these couplings (details discussed in the Supporting Information). New equations pertaining to $^2J_{HH}$ and $^3J_{HH}$ have been applied to the analysis of hydroxymethyl group *J*-couplings in several mono- and oligosaccharides, yielding information on C5−C6 and/or C6−O6 rotamer populations.

## Introduction

Oligosaccharides contain several conformational domains that must be defined in order to fully describe their three-dimensional structures and dynamics in solution. These domains, which include conformation of the constituent pyranosyl or furanosyl rings, *O*-glycoside linkage conformation, hydroxymethyl conformation, and C−O bond conformation (Chart 1),[1] are expected to be interdependent and to exhibit varied degrees of flexibility. Motions about *O*-glycosidic linkages defined by two C−O torsion angles, $\phi$ and $\psi$ (Chart 1), are frequently attributed to the $\psi$ torsion which, unlike $\phi$, is not subject to stereoelectronic control (e.g., the exoanomeric effect).[2] The more subtle C−O rotations are normally ignored, at least for molecules in solution, but these conformations are expected to play important roles in dictating structure and, presumably, reactivity in the bound state, where C−O bond rotations are either fixed or highly constrained, thereby enhancing lone-pair effects on C−H and C−C bond lengths.[3] Rotation of exocyclic C5−C6 bonds[4] (hydroxymethyl group conformation) modulates the hydrogen bonding characteristics of oligosaccharides (both intra- and intermolecular) and the dipole moment of the

**Chart 1. Conformational Domains of Oligosaccharides**[a]

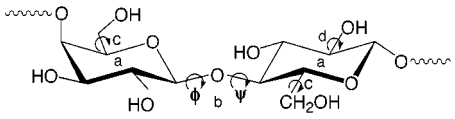


[a] Key: (a) ring conformation; (b) *O*-glycoside conformation; (c) hydroxymethyl group conformation; (d) exocyclic C−O bond conformation.

* To whom correspondence should be addressed.
[†] Swedish University of Agricultural Sciences.
[‡] Radiation Laboratory, University of Notre Dame.
[§] Stockholm University.
[||] Department of Chemistry and Biochemistry, University of Notre Dame.

(1) (a) Serianni, A. S. Nuclear Magnetic Resonance Approaches To Oligosaccharide Structure Elucidation. In *Glycoconjugates: Composition, Structure and Function*; Allen, H. J., Kisailus, E. C., Eds.; Marcel-Dekker: 1992; pp 71−102. (b) Serianni, A. S. In *Bioorganic Chemistry: Carbohydrates*; Hecht, S. M., Ed.; Oxford University Press: New York, 1999; pp 244−312.

(2) (a) Lemieux, R. U. *Pure Appl. Chem.* **1971**, *25*, 527−548. (b) Praly, J.-P.; Lemieux, R. U. *Can. J. Chem.* **1987**, *65*, 213−223. (c) Kirby, A. J. *The Anomeric Effect and Related Stereoelectronic Effects at Oxygen*; Springer-Verlag: Berlin, 1983. (d) Juaristi, E.; Cuevas, G. *The Anomeric Effect*; CRC Press: Boca Raton, 1995.

(3) (a) Serianni, A. S.; Wu, J.; Carmichael, I. *J. Am. Chem. Soc.* **1995**, *117*, 8645−8650. (b) Podlasek, C. A.; Stripe, W. A.; Carmichael, I.; Shang, M.; Basu, B.; Serianni, A. S. *J. Am. Chem. Soc.* **1996**, *118*, 1413−1425. (c) Kennedy, J.; Wu, J.; Drew, K.; Carmichael, I.; Serianni, A. S. *J. Am. Chem. Soc.* **1997**, *119*, 8933−8945. (d) Cloran, F.; Zhu, Y.; Osborn, J.; Carmichael, I.; Serianni, A. S. *J. Am. Chem. Soc.* **2000**, *122*, 6435−6448.

(4) (a) Rockwell, G. D.; Grindley, T. B. *J. Am. Chem. Soc.* **1998**, *120*, 10953−10963. (b) Bock, K.; Duus, J. O. *J. Carbohydr. Chem.* **1994**, *13*, 513−543.

10.1021/jo010985i CCC: $22.00 
Published on Web 01/11/2002

molecule (as does C−O rotation), both of which will affect overall physical and chemical properties.

Traditional assessments of oligosaccharide conformational domains by NMR have relied heavily on $^3J_{HH}$ (for ring conformations) and $^1H-^1H$ NOE (for linkage geometry), but these parameters are not without their limitations. For example, *O*-glycosidic linkage conformation cannot be assessed via $^3J_{HH}$, and inter-residue $^1H-^1H$ NOEs are frequently few in number and their interpretation complicated by the presence of significant resonance overlap that precludes reliable NOE measurements and/or by the presence of conformational averaging.[5] In general, and in contrast to most proteins, simple and complex saccharides cannot be considered rigid molecules, and therefore, observed NMR parameters will be averaged in a manner reflecting conformer populations in solution.[6] The shortage of experimental constraints has impeded progress in oligosaccharide conformational analysis and has led to a strong reliance on computational methods[7] to establish their solution conformations and dynamics.

The introduction of stable isotopes into saccharides offers opportunities to expand the repertoire of NMR experimental observables and thus address the problems described above. $^{13}$C-enrichment facilitates the measurement of *trans*-glycoside $^2J_{COC}$, $^3J_{COCH}$, and $^3J_{COCC}$ values which, when used collectively, can lead to assignments of preferred linkage conformation in oligosaccharides or, at a minimum, identify whether a given linkage is rigid or flexible.[8] Likewise, $^1J_{CC}$ values in HO−C−C−OH fragments in saccharides have been shown to depend not only on the C−C torsion angle but also on the C−O torsions;[9a] thus, when the former torsion is known, $^1J_{CC}$ can be a useful probe of the latter angles.[9b] In addition, $^{13}$C-enrichment enables the measurement of $J_{CH}$ and $J_{CC}$ values *within* furanosyl and pyranosyl rings. Being considerably more abundant than $^3J_{HH}$, these carbon-based *J*-couplings can be useful when investigating conformationally flexible structures.[10] In all of these cases, theoretical calculations of *J*-couplings proved invaluable in extending the inherently more limited experimental observations in order to provide a more detailed understanding of the relationships between specific scalar couplings and molecular structure.

Analysis of hydroxymethyl group conformation has relied heavily on $^3J_{HH}$ values to distinguish between the three potential staggered rotamers (Chart 2) and to estimate their populations in solution.[4] Despite the widespread use of this approach, data analysis frequently leads to questionable conclusions; for example, estimated populations of *tg* rotamers are often negative, an anomaly

**Chart 2. Idealized Rotamers about the C5−C6 Bond of Aldohexopyranosyl Rings**

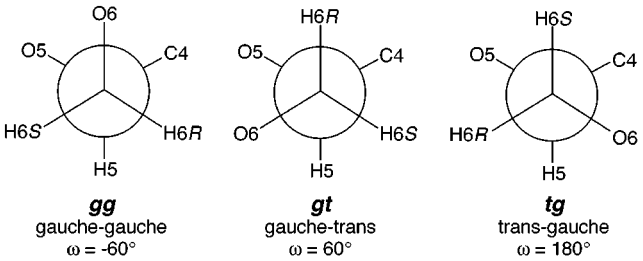


**Chart 3. *J*-Couplings Potentially Dependent on Exocyclic Hydroxymethyl Group Conformation in Aldohexopyranosyl Rings**

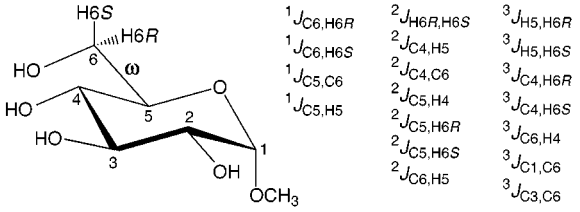


caused by the use of inappropriate standard values for the gauche and trans couplings.[4] In light of these difficulties, we have embarked on a systematic study of scalar couplings involving the hydroxymethyl protons and carbon in an effort to improve and/or develop additional experimental parameters on which to base conformational assignments in this conformationally flexible portion of saccharides. Eighteen *J*-couplings are available involving C5, C6 and their attached protons, and some of these are expected to exhibit a dependence on the C5−C6 torsion angle, $\omega$ (Chart 3); these couplings include $^3J_{H5,H6R}$, $^3J_{H5,H6S}$, $^3J_{C4,H6R}$, and $^3J_{C4,H6S}$. Many of the 14 remaining couplings are also likely to be useful conformational constraints. For example, while $^3J_{C1,C6}$ and $^3J_{C3,C6}$ depend mainly on the C1−O5−C5−C6 and C3−C4−C5−C6 torsion angles, respectively, these vicinal $^{13}C-^{13}C$ couplings are also sensitive to $\omega$ due to known effects of in-plane electronegative substituents (in these cases, O6) on coupling magnitude. Similar arguments can be made for the $^2J_{HH}$, $^2J_{CH}$, $^1J_{CC}$, and $^2J_{CC}$ values. The development of new NMR parameters for the determination of hydroxymethyl group conformation is particularly important for studies of oligosaccharides containing glycosidic linkages involving O6. In these structures, the two torsion angles $\phi$ and $\psi$, and a third torsion $\omega$ (defined as the O5−C5−C6−O6 torsion angle), determine linkage conformation, and a means to better assess $\omega$ is essential to assigning linkage conformation and mobility.

In this report, we present the results of studies of $^3J_{HH}$, $^2J_{HH}$, and $^1J_{CH}$ in hydroxymethyl group fragments, using experimental and theoretical (density functional theory, DFT) methods. Using several compounds containing constrained C−C and C−O torsion angles, we first sought to establish experimentally a set of limiting *J*-couplings for specific conformations about the C5−C6 ($\omega$) and C6−O6 ($\theta$) bonds. DFT methods were then applied to calculate $^3J_{H5,H6R}$ and $^3J_{H5,H6S}$ values in model compounds for comparison to the experimental couplings and to corresponding values predicted from an empirically determined generalized Karplus equation.[11] The latter comparisons

(5) Homans, S. W. *Prog. NMR Spectrosc.* **1990**, *22*, 55−81.
(6) Jardetzky, O. *Biochim. Biophys. Acta* **1980**, *621*, 227−232.
(7) Bush, C. A.; Martin-Pastor, M. *Annu. Rev. Biophys. Biomol. Struct.* **1999**, *28*, 269−293.
(8) (a) Church, T.; Serianni, A. S. *Carbohydr. Res.* **1996**, *280*, 177−186. (b) Serianni, A. S.; Bondo, P. B.; Zajicek, J. *J. Magn. Reson. Ser. B* **1996**, *112*, 69−74. (c) Basu, B.; Zhao, S.; Bondo, P.; Bondo, G.; Cloran, F.; Carmichael, I.; Stenutz, R.; Hertz, B.; Serianni, A. S. *J. Am. Chem. Soc.* **1998**, *120*, 11158−11173. (d) Cloran, F.; Carmichael, I.; Serianni, A. S. *J. Am. Chem. Soc.* **1999**, *121*, 9843−9851. (e) Cloran, F.; Carmichael, I.; Serianni, A. S. *J. Am. Chem. Soc.* **2000**, *122*, 396−397.
(9) (a) Carmichael, I.; Chipman, D. M.; Podlasek, C. A.; Serianni, A. S. *J. Am. Chem. Soc.* **1993**, *115*, 10863−10870. (b) Norrild, J. C.; Eggert, H. *J. Am. Chem. Soc.* **1995**, *117*, 1479−1484.
(10) (a) Podlasek, C. A.; Wu, J.; Stripe, W. A.; Bondo, P. B.; Serianni, A. S. *J. Am. Chem. Soc.* **1995**, *117*, 8635−8644. (b) Church, T. J.; Carmichael, I.; Serianni, A. S. *J. Am. Chem. Soc.* **1997**, *119*, 8946−8964.
(11) Haasnoot, C. A. G.; de Leeuw, F. A. A. M.; Altona, C. *Tetrahedron* **1980**, *36*, 2783−2792.

**Chart 4**

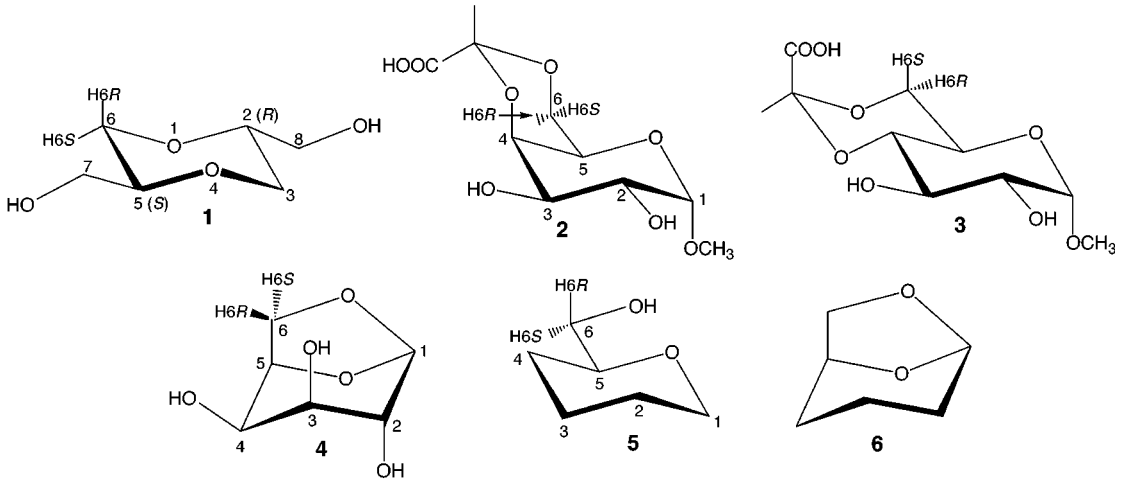


**Chart 5**

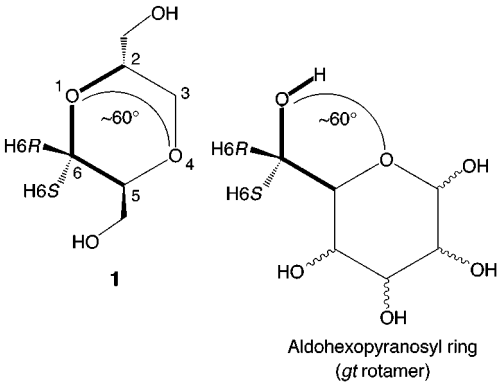


were made to determine the accuracy of the DFT-calculated *J*-couplings prior to extending the calculations to studies of the structural dependencies of $^2J_{H6R,H6S}$ and $^1J_{C6,H6R/S}$, about which considerably less is known. This work therefore provides the foundation for future studies of the remaining couplings identified in Chart 3. New equations relating $^2J_{H6R,H6S}$ and $^3J_{H5,H6R/S}$ are proposed that correlate these couplings with $\omega$ and/or $\theta$, and these equations are used to estimate C5−C6 and C6−O6 rotamer populations in several mono-, di-, and trisaccharides. Some progress has been made at interpreting $^1J_{CH}$ behavior in $CH_2OH$ fragments, although in this case correlations with molecular structure could not be firmly established.

## Experimental Section

**Compounds.** *trans*-2,5-Bis(hydroxymethyl)-1,4-dioxane (**1**) (Chart 4) was prepared according to Summerbell and Stephens.[12] Methyl 4,6-*O*-[(*R*)-1-carboxyethylidene]-α-D-galactopyranoside (**2**) and methyl 4,6-*O*-[(*S*)-1-carboxyethylidene]-α-D-glucopyranoside (**3**) (Chart 4) were prepared as described previously.[13] The torsion angles in **1**−**4** were calculated using the MM2 force field as implemented in Chem3D Pro Version 4.0 (CambridgeSoft Corp., Cambridge, MA, 1997) and were optimized to a root mean square (rms) gradient of 0.01 kcal/mol.

**NMR Spectroscopy.** One-dimensional $^1$H and $^{13}$C NMR spectra of **1**−**3** (50 mM in $^2H_2O$, 30°, pD 8 for **2**−**3**) were obtained on a Varian Unity*Plus* FT-NMR spectrometer (599.887 MHz for $^1$H, 150.860 MHz for $^{13}$C) with sufficient digital resolution to ensure errors ≤0.1 Hz in the measured *J*-couplings. $^1J_{CH}$ values were determined from coupled $^{13}$C−$^1$H gHSQC spectra, and the experimental error is estimated to be ∼1 Hz.

***J*-Coupling Calculations.** Specific staggered hydroxymethyl rotamers (nine structures) of model compound **5** (Chart 4), generated by systematically rotating the O5−C5−C6−O6 ($\omega$) and C5−C6−O6−O6H ($\theta$) torsions, were constructed in Chem3D and subsequently geometrically optimized using MM2. These initial structures were then imported into Gaussian94[14] and fully re-optimized (i.e., with no structural constraints) using density functional theory (DFT) with the B3LYP functional[15] and the 6-31G* basis set[16] (B3LYP/6-31G*).

Eclipsed rotamers (nine structures) were optimized by holding $\omega$ at fixed values (0°, 120°, −120°) and $\theta$ at fixed perfectly staggered values (60°, −60°, 180°). In these eclipsed conformers, $\omega$ and $\theta$ were held constant and the remaining degrees of freedom were optimized.

Coupling constants in **5** ($^2J_{H6R,H6S}$, $^3J_{H5,H6R}$, $^3J_{H5,H6S}$, $^1J_{C5,H5}$, $^1J_{C6,H6R}$, and $^1J_{C6,H6S}$) were calculated by DFT using a modified version of Gaussian94[14] and an extended basis set ([5s2p1d|3s1p]) designed to recover the Fermi contact contribution to the coupling. Earlier work in this laboratory made use of a [5s2p1d|2s] basis set to calculate $J_{CH}$ and $J_{CC}$ values in saccharides using DFT. This approach yielded calculated couplings within 5−10% of the actual values. However, the application of this basis set to $J_{HH}$ calculations gave larger errors, leading to the development of the [5s2p1d|3s1p] basis set used in this work. The [3s1p] contracted Gaussian basis for $^1$H provides a more flexible description of the valence space compared to the previously employed [2s] set (which was used for economy when the aim was to calculate $^{13}$C−$^{13}$C spin-couplings) and adds a polarizing p-function. As demonstrated herein, this extended basis set yields nearly quantitative results for $J_{HH}$; its impact on calculated $J_{CH}$ and $J_{CC}$ values, however, appears to be negligble.

Geometric optimizations and *J*-coupling calculations on model compounds **1** and **6** (Chart 4) were conducted in a fashion similar to that described for **5**.

(12) Summerbell, R. K.; Stephens, J. R. *J. Am. Chem. Soc.* **1954**, *76*, 6401−6407.

(13) Jansson, P.-E.; Lindberg, J.; Widmalm, G. *Acta Chem. Scand.* **1993**, *47*, 711−715.

(14) Frisch, M. J.; Trucks, G. W.; Schlegel, H. B.; Gill, P. M. W.; Johnson, B. G.; Robb, M. A.; Cheeseman, J. R.; Keith, T.; Petersson, G. A.; Montgomery, J. A.; Raghavachari, K.; Al-Laham, M. A.; Zakrzewski, V. G.; Ortiz, J. V.; Foresman, J. B.; Peng, C. Y.; Ayala, P. Y.; Chen, W.; Wong, M. W.; Andres, J. L.; Replogle, E. S.; Gomperts, R.; Martin, R. L.; Fox, D. J.; Binkley, J. S.; Defrees, D. J.; Baker, J.; Stewart, J. P.; Head-Gordon, M.; Gonzalez, C.; Pople, J. A. *Gaussian94*; Gaussian, Inc.: Pittsburgh, PA, 1995.

(15) Becke, A. D. *J. Chem. Phys.* **1993**, *98*, 5648−5652.

(16) Hehre, W. J.; Ditchfield, R.; Pople, J. A. *J. Chem. Phys.* **1972**, *56*, 2257−2261.

**Table 1. Torsion Angles,[a] $\omega$ and $\theta$, and Experimental $^2J_{HH}$, $^3J_{HH}$, and $^1J_{CH}$ Values[b] in Conformationally Constrained 1−4**

| compd | $\omega$[d] | $\theta$[e] | $^2J_{H6R,H6S}$ | $^3J_{H5,H6R}$ | $^3J_{H5,H6S}$ | $^1J_{C6,H6R}$ | $^1J_{C6,H6S}$ |
|---|---|---|---|---|---|---|---|
| **1** | +58 | −58 | −11.7 | 10.7 | 2.5 | 142 | 146 |
| **2** | −69 | −58 | −13.1 | 1.8 | 1.8 | 143 | 153 |
| **3** | −178 | 57 | −10.6 | 5.0 | 10.3 | 152 | 142 |
| **4**[c] | −33 | 9 | −7.6 | 0.8 | 5.2 | | |

[a] In degrees. [b] In Hz, ± 0.1 Hz, in $^2H_2O$, 30 °C. [c] Torsion angles were obtained from the crystal structure,[25] and $J_{HH}$ values were taken from ref 26. [d] Defined as O5−C5−C6−O6 in **2**−**4** and O4−C5−C6−O1 in **1**. [e] Defined as C5−C6−O6−CX in **2**−**4** and C5−C6−O1−C2 in **1**.

Equations 1−3 were derived from the calculated couplings determined in **5** and **6** using a least-squares procedure. The O5−C5−C6−O6 torsion angle ($\omega$) was used to derive all equations since using the H5−C5−C6−H6*R*/*S* torsion angle as the reference angle did not improve the rms errors. Differences in the observed *J*-couplings and those calculated from eqs 1−3 did not appear to follow any simple pattern that would justify the inclusion of additional terms in these equations.

Hypersurfaces were generated from a sequence of calculations (B3LYP/6-31G*) performed over a uniform grid of 30° increments in both $\omega$ and $\theta$. This increment gave satisfactory hypersurfaces while keeping computational costs within reasonable bounds. At each grid point, all other geometric parameters were relaxed and the corresponding spin−spin coupling constants calculated as described above.

## Results and Discussion

**(a) Choice of Model Compounds.** Compounds **1** (2*R*,5*S*-bis[hydroxymethyl]-1,4-dioxane), **2** (methyl 4,6-[(*R*)-1-carboxyethylidene]-α-D-galactopyranoside), and **3** (methyl 4,6-[(*S*)-1-carboxyethylidene]-α-D-glucopyranoside) (Chart 4) were chosen as models for the *gt*, *gg*, and *tg* rotamers, respectively, of the C5−C6 bond of aldohexopyranosyl rings. Compound **4** (1,6-anhydro-β-D-galactopyranose) (Chart 4) was included to test if conclusions drawn from staggered rotamers are applicable to nonstaggered rotamers.

For the DFT calculations, compound **5** (2-hydroxymethyltetrahydropyran) (Chart 4) was selected as a model of the flexible C5−C6 bond of aldohexopyranosyl rings. Limited calculations were also performed on compounds **1** and **6** (7,8-dioxabicyclo[3.2.1]octane), the latter being a model of compound **4**.

**(b) Vicinal (Three-Bond) $^1$H−$^1$H Coupling Constants.** Two $^3J_{HH}$ values are sensitive to $\omega$, and an experimentally derived Karplus equation[11] has been used previously to correlate these vicinal couplings with H−C−C−H torsion angles. An evaluation of the dependencies of these couplings on both $\omega$ and $\theta$ was sought by measuring $^3J_{HH}$ values in compounds **1**−**4** containing constrained hydroxymethyl fragments and obtaining theoretical *J*-couplings from DFT calculations on compounds **5** and **6**.

In **1** (*gt* model), $^3J_{H5,H6R}$ and $^3J_{H5,H6S}$ are 10.7 and 2.5 Hz, respectively, corresponding to H−C−C−H torsion angles of ∼178° and ∼58°, respectively (Table 1). To our knowledge, compound **1** is the first conformationally constrained mimic of a *gt* rotamer (Chart 5) in which $^3J_{HH}$ values have been measured.[17] More importantly, these observed $^3J_{H5,H6R}$ and $^3J_{H5,H6S}$ values are identical to those proposed for this rotamer by Bock and Duus.[4b] In **2** (*gg* model), $^3J_{H5,H6R}$ and $^3J_{H5,H6S}$ are both 1.8 Hz despite the difference in H−C−C−H torsion angles (∼51° and ∼69°, respectively) (Table 1). $^3J_{H5,H6R}$ and $^3J_{H5,H6S}$ values in **3** (*tg* model) are 5.0 and 10.3 Hz, respectively, and correspond to H−C−C−H torsion angles of ∼58° and ∼178°, respectively (Table 1).

Taken collectively, these results suggest that values of $^3J_{HH(anti)}$ are essentially the same in the *gt* and *tg* rotamers (10.3 and 10.7 Hz for an ∼178° torsion angle) but $^3J_{HH(gauche)}$ values vary widely. For example, couplings of 2.5 and 5.0 Hz are observed in **1** and **3**, respectively, for torsion angles of ∼60°, while couplings of 1.8 Hz are observed in **2** for torsion angles of ∼51° and ∼69°. Thus, $^3J_{HH(gauche)}$ of 1.8−5.0 Hz are observed in hydroxymethyl group fragments over a relatively narrow range of H−C−C−H torsion angles (∼50°−70°). This problem stems partly from the effect of electronegative substituents (O5 or O6) on these gauche couplings;[18] for example, $^3J_{H5,H6R}$ in **2** is expected to be reduced in magnitude due to the antiperiplanar relationship between H5 and O6 and H6*R* and O5. Thus, errors associated with the analysis of $^3J_{HH}$ in hydroxymethyl fragments are more likely to arise from the use of inappropriate standard $^3J_{HH(gauche)}$ values than from inappropriate standard $^3J_{HH(anti)}$ values.

The interpretation of $^3J_{HH}$ in **4** is complicated by the presence of strain in the molecule. This notwithstanding, $^3J_{H5,H6R}$ and $^3J_{H5,H6S}$ values of 0.8 and 5.2 Hz correspond to H−C−C−H torsion angles of ∼87° and ∼33°, respectively. The latter coupling is smaller than expected, given the 5.0 Hz coupling in **3** for a torsion angle of ∼62°. This observation reinforces the above-noted conclusions regarding standard values of $^3J_{HH(gauche)}$.

The $^3J_{HH}$ values in 2-hydroxymethyl-tetrahydropyran **5** were calculated as a function of $\omega$ and $\theta$ (Table 2) using density functional theory (DFT), from which Karplus equations were derived for comparison to the experimentally derived equation.[11] The latter comparison provided a means of validating the DFT method for the computation of $^3J_{HH}$ values in order to justify its subsequent application to studies of $^2J_{H6R,H6S}$ and $^1J_{C6,H6R/S}$ (see below). Further validation was obtained by comparing computed $^2J_{HH}$ and $^3J_{HH}$ values in the conformationally constrained 1,6-anhydropyranose model compound **6** to corresponding experimental couplings observed in **4**. The experimental and computed couplings (Tables 1 and 2, respectively) are in very good agreement. The largest deviation (0.5 Hz) may arise, in part, from relatively small differences in torsion angles; for example, the 33° torsion angle associated with $^3J_{H5,H6S}$ in **4** lies on a steep portion of the Karplus curve where small changes in torsion angle translate into relatively large changes in $^3J_{HH}$.

*J*-couplings were also computed in **1** (O1/O4 trans to O8/O7; C2/C5 trans to O8H/O7H; Chart 4), yielding the

(17) The preparation of a rigid *gt* model compound has been claimed (Köpper, S.; Brandenberg, A. *J. Carbohydr. Chem.* **1993**, *12*, 801−804), but the reported $^3J_{H5,H6R}$ (9.5 Hz) and $^3J_{H5,H6S}$ (1.5 Hz) suggest that the geometry is either distorted or conformationally averaged.

(18) Günther, H. *NMR Spectroscopy*; J. Wiley and Sons: New York, 1995; p 119.

**Table 2. Torsion Angles,[a] $\omega$ and $\theta$, and Calculated $^2J_{HH}$, $^3J_{HH}$, and $^1J_{CH}$ Values[b] in 5 and 6**

| compd | $\omega$[c] | $\theta$[d] | $^2J_{H6R,H6S}$ | $^3J_{H5,H6R}$ | $^3J_{H5,H6S}$ | $^1J_{C5,H5}$ | $^1J_{C6,H6R}$ | $^1J_{C6,H6S}$ | C5−C6 rotamer[e] |
|---|---|---|---|---|---|---|---|---|---|
| **5** | 62 | 57 | −12.5 | 10.7 | 1.7 | 135 | 147 | 138 | *gt* |
| | 57 | −48 | −11.3 | 10.7 | 2.7 | 142 | 143 | 143 | |
| | 72 | 192 | −8.6 | 9.5 | 1.1 | 142 | 140 | 139 | |
| | −58 | 50 | −11.3 | 0.8 | 2.7 | 139 | 143 | 145 | *gg* |
| | −70 | −72 | −13.1 | 1.7 | 1.6 | 136 | 136 | 149 | |
| | −72 | 171 | −8.5 | 2.1 | 1.6 | 136 | 137 | 143 | |
| | 176 | 74 | −12.1 | 4.8 | 10.9 | 142 | 150 | 141 | *tg* |
| | 177 | −69 | −11.9 | 3.9 | 11.3 | 135 | 144 | 147 | |
| | 176 | 176 | −6.8 | 4.3 | 10.9 | 141 | 144 | 141 | |
| | 120 | 60 | −12.9 | 0.9 | 3.3 | 139 | 148 | 140 | |
| | 120 | −60 | −12.9 | 1.2 | 2.9 | 140 | 144 | 144 | |
| | 120 | 180 | −8.5 | 1.0 | 3.1 | 143 | 144 | 139 | |
| | 0 | 60 | −11.9 | 5.8 | 7.6 | 139 | 145 | 140 | |
| | 0 | −60 | −11.9 | 4.9 | 8.8 | 141 | 140 | 145 | |
| | 0 | 180 | −7.6 | 5.3 | 8.6 | 139 | 139 | 139 | |
| | −120 | 60 | −13.6 | 8.4 | 2.5 | 140 | 145 | 146 | |
| | −120 | −60 | −13.5 | 7.3 | 3.2 | 139 | 141 | 150 | |
| | −120 | 180 | −9.3 | 8.0 | 2.8 | 139 | 139 | 145 | |
| **6** | −31 | 6 | −7.7 | 0.6 | 4.7 | | 146 | 144 | |

[a] In degrees. [b] In Hz. [c] Defined as O5−C5−C6−O6 in **5** and **6**. [d] Defined as C5−C6−O6−HO6 in **5** and C5−C6−O6−C1 in **6**. [e] Defined in Chart 2.

following data: $^1J_{C5,H5} = 144.5$ Hz; $^3J_{H5,H6R} = 11.0$ Hz; $^3J_{H5,H6S} = 2.6$ Hz; $^2J_{H6R,H6S} = -11.5$ Hz; $^1J_{C6,H6R} = 140.3$ Hz; $^1J_{C6,H6S} = 150.6$ Hz. The computed $^3J_{HH}$ are again in good agreement with experimental values (Table 1). Differences between the experimental and calculated $^1J_{CH}$ are attributed to the effect of *exocyclic* hydroxymethyl group averaging in **1** in solution (see below).

For $\omega = 180°$ (*tg* rotamer), the effect of C6−O6 rotation on the computed $^3J_{H5,H6R}$ and $^3J_{H5,H6S}$ values in **5** is small (0.4−0.9 Hz) (Table 2). Slightly larger effects of C6−O6 bond rotation are observed for $\omega = 60°$ and −60°, ranging from 1.1 to 1.6 Hz. As expected, the main determinant of these couplings is the H−C−C−H torsion angle, and if the small effect of $\theta$ on these couplings (possibly caused by oxygen lone-pair effects on C−H bond lengths; see below) is ignored, two theoretical equations (eqs 1 and 2) can be derived from the computed couplings in **5** and **6** (Table 2) that relate $^3J_{H5,H6R}$ and $^3J_{H5,H6S}$ to $\omega$:

$$^3J_{H5,H6R} = 5.08 + 0.47\cos(\omega) + 0.90\sin(\omega) - 0.12\cos(2\omega) + 4.86\sin(2\omega) \quad (1)$$

$$^3J_{H5,H6S} = 4.92 - 1.29\cos(\omega) + 0.05\sin(\omega) + 4.58\cos(2\omega) + 0.07\sin(2\omega) \quad (2)$$

Using eqs 1 and 2, plots of theoretical $^3J_{H5,H6R}$ and $^3J_{H5,H6S}$ values vs $\omega$ were constructed and superimposed on corresponding plots generated from couplings predicted by a generalized Karplus equation[11] (Figure 1). The two data sets are in excellent agreement. The experimental *J*-couplings obtained in **1**−**4** (Table 1), which have constrained $\omega$ values, are also in good agreement with the calculated couplings (Figure 1).

The rms deviations (Table 3) between eqs 1 and 2 and the calculated (in **5** and **6**) and experimental (in **1**−**4**) couplings are ~0.5 Hz. This deviation compares favorably with the reported standard deviation of 0.5 Hz for the generalized Karplus equation. In addition, optimization of the former equations using the H5−C5−C6−H6 torsion angles in **5** failed to reduce this error. It therefore appears that 0.5 Hz is the limit of accuracy that can be expected from $^3J_{HH}$ Karplus-type equations based on considerations of only the $\omega$ torsion angle.

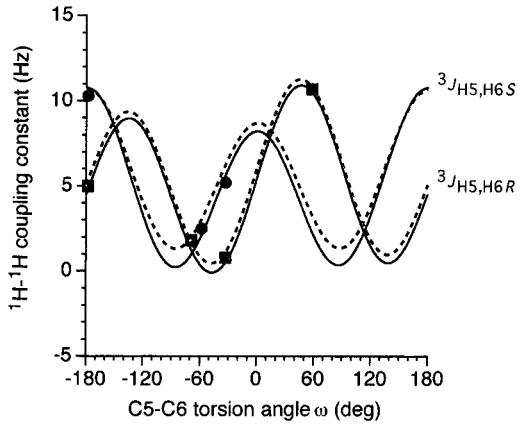


**Figure 1.** Plots of the dependencies of calculated $^3J_{H5,H6R}$ and $^3J_{H5,H6S}$ in **5** on the O5−C5−C6−O6 torsion angle, $\omega$, derived from eqs 1 and 2 (solid lines) and from the Haasnoot/Altona generalized Karplus equation[11] (dashed lines). Experimental data taken from Table 1 are shown in squares ($^3J_{H5,H6R}$) and circles ($^3J_{H5,H6S}$).

**Table 3. Root-Mean-Square Deviations[a] in Equations 1−3 and the Calculated Couplings[b] in 5 and Experimental Couplings[c] in 1−4**

| equation | calcd[d] | exptl[e] |
|---|---|---|
| 1 ($^3J_{H5,H6R}$) | 0.5 (0.6)[f] | 0.3 |
| 2 ($^3J_{H5,H6S}$) | 0.6 (0.6)[f] | 0.5 |
| 3 ($^2J_{H6R,H6S}$) | 0.8 | 0.9 |

[a] In Hz. [b] Data from Table 2. [c] Data from Table 1. [d] $n = 18$. [e] $n = 4$. [f] As a function of the H5−C5−C6−H6*R*/*S* torsion angle only.

**(c) Geminal (Two-Bond) $^1$H−$^1$H Coupling Constants.** $^2J_{H6R,H6S}$ values in **1**−**4** range from −7.6 Hz in **4** to −13.1 Hz in **2** (Table 1). An important factor influencing this *J*-coupling is the H−C−H bond angle. In general, more negative couplings are associated with smaller H−C−H bond angles for $sp^3$-hybridized carbon,[19] suggesting that H−C−H bond angles increase in the order **2** > **3** > **4**, all else being equal. This analysis assumes

**Table 4. Selected Calculated Bond Lengths[a] and Angles[b] in 5 as a Function of $\omega$ and $\theta$**

| $\omega^c$ | $\theta^d$ | $\angle_{H6R-C6-H6S}$ | $r_{C5-H5}$ | $r_{C6-H6R}$ | $r_{C6-H6S}$ |
|---|---|---|---|---|---|
| 62 | 57 | 107.8 | 1.1100 | 1.0946 | 1.1036 |
| 57 | −48 | 108.0 | 1.1044 | 1.1031 | 1.0953 |
| 72 | 192 | 108.0 | 1.1049 | 1.1008 | 1.1031 |
| −58 | 50 | 108.1 | 1.1054 | 1.0952 | 1.1017 |
| −70 | −72 | 107.9 | 1.1079 | 1.1027 | 1.0940 |
| −72 | 171 | 108.0 | 1.1076 | 1.1033 | 1.1002 |
| 176 | 74 | 107.6 | 1.1048 | 1.0936 | 1.1011 |
| 177 | −69 | 107.6 | 1.1094 | 1.1000 | 1.0945 |
| 176 | 176 | 107.8 | 1.1050 | 1.1002 | 1.1015 |
| 120 | 60 | 107.9 | 1.1060 | 1.0926 | 1.1022 |
| 120 | −60 | 107.9 | 1.1059 | 1.0998 | 1.0946 |
| 120 | 180 | 108.0 | 1.1032 | 1.0992 | 1.1018 |
| 0 | 60 | 107.0 | 1.1064 | 1.0952 | 1.1022 |
| 0 | −60 | 107.0 | 1.1052 | 1.1035 | 1.0938 |
| 0 | 180 | 106.9 | 1.1060 | 1.1030 | 1.1019 |
| −120 | 60 | 107.7 | 1.1054 | 1.0935 | 1.0994 |
| −120 | −60 | 107.7 | 1.1060 | 1.1010 | 1.0923 |
| −120 | 180 | 107.8 | 1.1054 | 1.1010 | 1.0988 |

[a] In Å. [b] In degrees. [c] Defined as O5−C5−C6−O6. [d] Defined as C5−C6−O6−HO6.

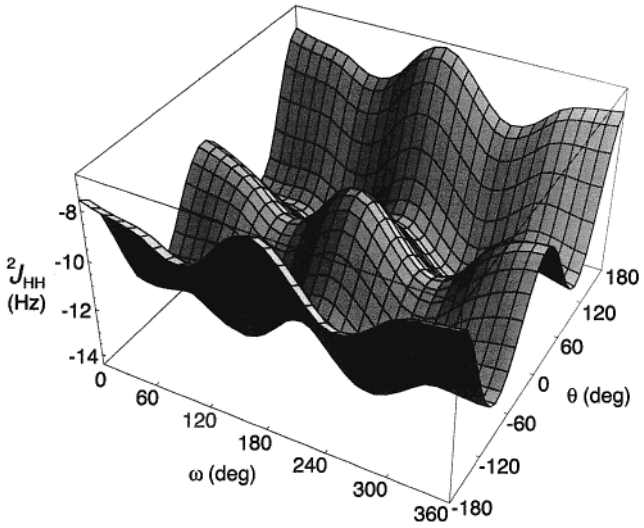


**Figure 2.** The 3D hypersurface generated from $^2J_{H6R,H6S}$ couplings computed in **5** and plotted as a function of $\omega$ and $\theta$.

that $\omega$ and/or $\theta$ do not affect $^2J_{HH}$; we show below that $\theta$ affects this coupling more significantly than the H−C−H bond angle.

Computed $^2J_{HH}$ values in **5** and **6** (Table 2) vary substantially in magnitude and are influenced more by $\theta$ than by $\omega$; the H6*R*−C6−H6*S* bond angle cannot be a factor here since it remains nearly constant (107.7 ± 0.4°) in the optimized structures (Table 4). $^2J_{HH}$ increases by ∼4 Hz upon rotation of $\theta$ from C5−O6H gauche to C5−O6H trans. Treatment of the computed $^2J_{HH}$ in Table 2 yielded eq 3 which relates $^2J_{HH}$ to $\omega$ and $\theta$:

$$^2J_{H6R,H6S} = 0.76\cos(\omega) - 2.02\cos(\theta) - 11.26 \quad (3)$$

The relatively small rms deviation between eq 3 and the calculated and experimental couplings (Table 3) is consistent with the observed 3D hypersurface obtained from plots of $^2J_{HH}$ vs these torsions (Figure 2). Slices through the surface parallel to either axis yield very similar 2D curves, indicating relatively constant functions for $\omega$ and $\theta$; indeed, the full hypersurface is symmetric, with data in one quadrant sufficient to generate the complete surface.

Equation 3 contains two independent variables, but $\omega$ can be evaluated from eqs 1 and 2, thereby allowing an estimation of the C6−O6 torsion angle from eq 3. For a freely rotating C6−O6 bond, a value of ∼−11 Hz is estimated for $^2J_{H6R,H6S}$. Smaller observed couplings (absolute values) suggest a preference for the rotamer having C5 trans to O6H.

**(d) One-Bond $^{13}$C−$^1$H Coupling Constants.** C−H bond length is a key determinant of $^1J_{CH}$ values in saccharides, with shorter bonds (greater *s*-character) yielding larger couplings.[3a] Several structural factors influence C−H bond length in aldopyranosyl rings: axial vs equatorial bond orientation, vicinal lone-pair effects,[3a,b] 1,3-lone-pair effects,[3c] and 1,4-lone-pair effects.[3d] In **1**−**3**, the axial hydroxymethyl C6−H6 bond displays the smaller $^1J_{CH}$ (Table 1), as expected since axial C−H bonds are normally longer than equatorial C−H bonds.[20a−d] This orientational effect is reinforced by vicinal antiperiplanar oxygen lone-pair interactions that further lengthen the axial C6−H6 bonds[3a,b] and/or by 1,3-lone-pair effects[3c] that shorten the equatorial C6−H6 bonds.[21]

Whereas a separation of the different structural effects on bond length, and hence $^1J_{CH}$, is not feasible for compounds **1**−**3**, this analysis is possible for the calculated $^1J_{CH}$ in **5** (Tables 2 and 4). The effects of 1,3-interactions with oxygen lone-pairs are observed on $r_{C5,H5}$ and $^1J_{C5,H5}$ since the orientation of the vicinal lone-pairs on O5 and the orientation of the C5−H5 bond (axial) remain fixed in all structures. If exceptions are made for two conformations (57°, −48°; −58°, 50°) that contain H-bonding between O6H and O5, then $r_{C5,H5}$ and $^1J_{C5,H5}$ values can be divided into two groups. In the presence of a 1,3-interaction with an O6 lone-pair, $r_{C5,H5}$ varies from 1.1048 to 1.1050 Å, giving $^1J_{C5,H5}$ values ranging from 141 to 142 Hz. In the absence of this interaction, $r_{C5,H5}$ increases to 1.1076−1.1100 Å and $^1J_{C5,H5}$ values decrease by ∼6 Hz to 135−136 Hz.[22] A plot of calculated $^1J_{C5,H5}$ vs $r_{C5,H5}$ is reasonably linear (Figure 3A), indicating that C−H bond length is highly correlated with $^1J_{CH}$ magnitude, with shorter bonds yielding larger couplings.

The relationship between $r_{C6,H6}$, $^1J_{C6,H6}$ and hydroxymethyl group conformation is not as straightforward to

(19) Maciel, G. E.; McIver, J. W.; Ostlund, N. S.; Pople, J. A. *J. Am. Chem. Soc.* **1970**, *92*, 4151.

(20) (a) In cyclohexane rings, it is generally held[20b] that an equatorial group X will show a C−X stretching vibration at a higher frequency than will the corresponding axial group (exceptions to this correlation have been observed in some substituted rings). From Badger's rule,[20c,d] the equatorial C−X bond length is expected to be shorter than the corrresponding axial C−X bond length. (b) Eliel, E. L.; Allinger, N. L.; Angyal, S. J.; Morrison, G. A. *Conformational Analysis*; Interscience Publishers: New York, 1965; pp 143−144. (c) Badger, R. M. *J. Chem. Phys.* **1934**, *2*, 128−131. (d) Badger, R. M. *J. Chem. Phys.* **1935**, *3*, 710−714.

(21) For example, in **2** (*gg* rotamer), $^1J_{C6,H6R}$ is ∼10 Hz smaller than $^1J_{C6,H6S}$ (Table 1). This difference is caused by two factors: C−H bond orientation and oxygen lone-pair effects on C−H bond lengths. The equatorial C6−H6*S* bond is expected to be shorter than the axial C6−H6*R* bond (orientation effect), leading to a larger $^1J_{CH}$ in the former. The O6 lone-pair antiperiplanar to the C6−H6*R* bond leads to further lengthening of this bond (vicinal lone-pair effect), and a 1,3-effect between a lone-pair on O5 and H6*S* shortens the C6−H6*S* bond, leading to a further enhancement of the *difference* between $^1J_{C6,H6R}$ and $^1J_{C6,H6S}$. All of these structural factors are reinforcing (i.e., all lead to shortening of the C6−H6*S* bond and lengthening of the C6−H6*R* bond), thereby yielding a maximum difference between the $^1J_{CH}$ values. In **3** (*tg* rotamer), $^1J_{C6,H6R}$ is ∼10 Hz larger than $^1J_{C6,H6S}$ (Table 1), and this difference is attributed to only bond orientation and vicinal lone-pair factors (1,3-lone-pair effects from O5 are experienced by both the C6−H6*R* and C6−H6*S* bonds and are expected to cancel).

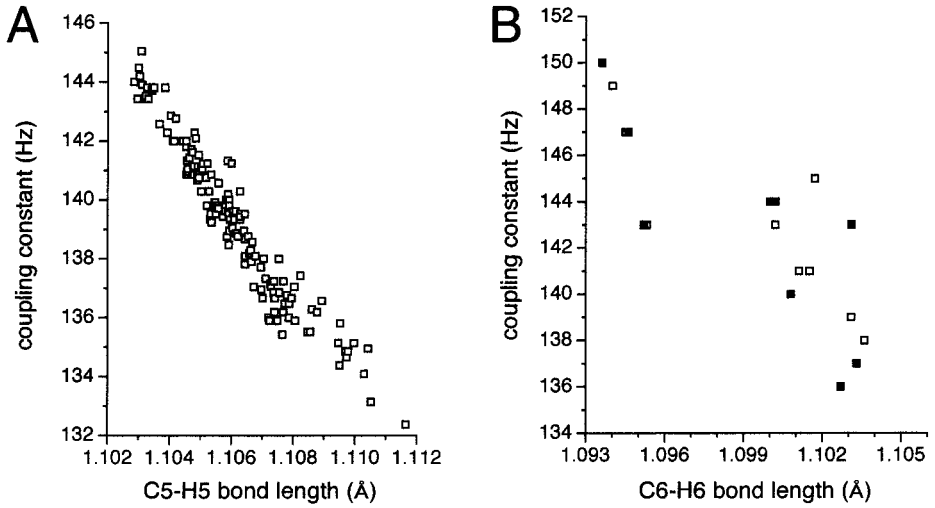


**Figure 3.** (A) Computed $^1J_{C5,H5}$ vs C5−H5 bond length, and (B) computed $^1J_{C6,H6}$ vs C6−H6 bond length, in **5**. Data were generated from systematic rotations about $\omega$ and $\theta$.

discern since bond orientation, vicinal lone-pair interactions with O6 and 1,3-interactions with O5 have to be considered. The shortest C6−H6 bonds, and hence the largest $^1J_{C6,H6}$ values, are expected for C6−H6 bonds that do not experience bond-lengthening vicinal (anti) O6 lone-pair interactions and experience bond-shortening 1,3-interactions with an O5 lone-pair. Four such C6−H6 bonds are found among the staggered conformers of **5**, with $r_{C6,H6} = 1.0942 \pm 0.0005$ Å and $^1J_{C6,H6} = 148 \pm 2$ Hz. On the opposite end of the scale are four C6−H6 bonds that experience bond-lengthening interactions with vicinal lone-pairs but lack bond-shortening 1,3-interactions. In these cases, $r_{C6,H6} = 1.1032 \pm 0.0004$ Å and $^1J_{C6,H6} = 138 \pm 1$ Hz. The remaining ten C6−H6 bonds lack either bond length altering interactions completely (two cases) or experience two opposing effects (eight cases), yielding $r_{C6,H6}$ (1.0999 ± 0.0026 Å) and $^1J_{C6,H6}$ (143 ± 2 Hz) that fall between the two above-mentioned extremes. Superimposed on these lone-pair effects is the effect of bond orientation; thus for two C6−H6 bonds experiencing the same lone-pair interactions, that having a (pseudo)equatorial orientation is expected to be shorter than that having a (pseudo)axial orientation. This orientational effect contributes to the small range of bond lengths in each of the above three categories. A plot of $r_{C6,H6}$ vs $^1J_{C6,H6}$ (Figure 3B) for staggered rotamers about $\omega$ and $\theta$ is reasonably linear. Data from two structures (57, −48; −58, 50; Tables 2 and 4) (four data points) in which H-bonding between O6H and O5 occurs account for the scatter; presumably this H-bonding perturbs the structures sufficiently to cause the observed deviations.

The above-noted structural factors affecting $^1J_{CH}$ lead to the finding that fitting the calculated $^1J_{CH}$ to only two torsion angles, $\omega$ and $\theta$, gives relatively large rms errors, thus precluding a quantitative treatment these couplings. Rotation of the C6−O6 bond modulates the stereoelectronic effect of the O6 lone-pairs on the C6−H6*R* and C6−H6*S* bond lengths, but other effects (e.g., 1,3-lone-pair interactions with O5 and bond orientation effects) also influence these bond lengths. Presumably the reported solvent dependence of $^1J_{CH}$ in saccharides[23] reflects differences in C−O torsional behavior. Further work on this problem is needed; a more detailed discussion of the $^1J_{CH}$ data, including semiquantitative equations relating these couplings to $\omega$ and $\theta$, is available in the Supporting Information.

**Table 5. Comparison of Limiting Values for $^3J_{H5,H6R}$ and $^3J_{H5,H6S}$ in the Three Staggered Rotamers about the C5−C6 Bond of Aldohexopyranosyl Rings**

| | coupling (Hz) | | | | | |
|---|---|---|---|---|---|---|
| | $^3J_{H5,H6R}$ | | | $^3J_{H5,H6S}$ | | |
| source | *gt* | *gg* | *tg* | *gt* | *gg* | *tg* |
| Nishida[a] | 10.8 | 1.7 | 4.1 | 2.4 | 2.2 | 11.1 |
| Manor[b] | 11.5 | 1.3 | 5.8 | 1.3 | 2.7 | 11.7 |
| Bock and Duus[c] | 10.7 | 0.9 | 5.5 | 2.5 | 2.2 | 10.7 |
| Compounds **1**−**3** | 10.7 | 1.8 | 5.0 | 2.5 | 1.8 | 10.3 |
| eqs 1 and 2[d] | 9.9 | 0.8 | 4.5 | 1.5 | 1.3 | 10.8 |

[a] Reference 27. [b] Reference 28. [c] Reference 4b. [d] Values of $\omega$: *gt*, +65°; *gg*, −65°; *tg*, 180°; these values were used to estimate rotamer populations in Table 7.

**(e) Applications to Specific Compounds.** Rotameric distributions about the C5−C6 bonds of aldohexopyranosyl rings can be determined[24a] from $^3J_{H5,H6R}$ and $^3J_{H5,H6S}$ if stereochemical assignments of the H6 signals are available. The limiting values of these couplings depend on assumptions made about the torsion angles and on the choice of Karplus equation. The limiting couplings in Tables 5 and 6 were used to estimate the percentages of C5−C6 and C6−O6 trans rotamers in several mono-, di- and trisaccharides **7**−**14** (Chart 6,

(22) C−H bond length shortening caused by oxygen 1,3-lone-pair effects is observed for the C5−H5 bond in **5** as a result of C6−O6 bond rotation. Thus, for $\omega = +57-72°$, $r_{C5,H5}$ is longer for $\theta = +57°$ than for $\theta = -48°$ or 192°, and $^1J_{C5,H5}$ (+62°, +57°) < $^1J_{C5,H5}$ (+57°,−48°) and $^1J_{C5,H5}$ (+72°, 192°) ($\Delta = 7$ Hz). Likewise, for $\omega = 176-177°$, $r_{C5,H5}$ is longer for $\theta = -69°$ than for $\theta = +74°$ and 176°, and $^1J_{C5,H5}$ (177°, −69°) < $^1J_{C5,H5}$ (176°, 74°) and $^1J_{C5,H5}$ (176°, 176°) ($\Delta = 6$ Hz). For $\omega = -58-72°$, there are no 1,3-lone-pair effects from O6 on the C5−H5 bond, and thus, $r_{C5,H5}$ is similar for $\theta = +50°$, −72°, and 171°, and $^1J_{C5,H5}$ values are more similar (137 ± 2 Hz).

(23) Bock, K.; Pedersen, C. *Carbohydr. Res.* **1979**, *71*, 319.

(24) (a) Percentages of *gt*, *gg*, and *tg* rotamers were calculated by solving the following three equations simultaneously: $^3J_{H5,H6R} = p_{gt}(^3J_{H5,H6R(gt)}) + p_{gg}(^3J_{H5,H6R(gg)}) + p_{tg}(^3J_{H5,H6R(tg)})$, $^3J_{H5,H6S} = p_{gt}(^3J_{H5,H6S(gt)}) + p_{gg}(^3J_{H5,H6S(gg)}) + p_{tg}(^3J_{H5,H6S(tg)})$, and $p_{gt} + p_{gg} + p_{tg} = 1$. In these equations, $p$ is the fraction of the respective rotamer, $^3J_{H5,H6R(gt)}$ is the standard value of $^3J_{H5,H6R}$ in the *gt* rotamer, $^3J_{H5,H6R(gg)}$ is the standard value of $^3J_{H5,H6R}$ in the *gg* rotamer, and so forth. Standard couplings used in the calculations were derived from eqs 1 and 2 (see Table 5). (b) Fraser, R. R.; Kaufman, M.; Morand, P.; Govil, G. *Can. J. Chem.* **1969**, *47*, 403−409. (c) Hayes, M. L.; Serianni, A. S.; Barker, R. *Carbohydr. Res.* **1982**, *100*, 87−101.

**Table 6. Limiting Values[a] for $^2J_{H6R,H6S}$ in the Three Staggered Rotamers about the C5−C6 Bond of Aldohexopyranosyl Rings**

| | C5−C6 rotamer | |
|---|---|---|
| coupling (Hz) | *gt*/*gg* | *tg* |
| C5−O6H gauche[b] | −12.7 | −11.5 |
| C5−O6H trans[c] | −9.7 | −8.5 |

[a] From eq 3. [b] $\theta = 60$ or $-60°$. [c] $\theta = 180°$.

Table 7). In these calculations, the distribution of C6−O6 rotamers was assumed to be similar in the three C5−C6 rotamers.

Comparisons of **7**−**9** illustrate the importance of C4 substitution on C5−C6 rotamer populations. In the 4-deoxypyranoside **7**, substantial percentages of all three rotamers are observed. Hydroxylation at C4 affects this distribution significantly, as expected; when O4 is equatorial (**8**), the *tg* rotamer population is reduced, whereas when O4 is axial (**9**), the *gg* population is reduced. These findings are consistent with earlier observations made in $^{13}$C-labeled saccharides[24c] where stereochemical assignments of the H6*R* and H6*S* signals were made through the analysis of complementary $^3J_{HH}$ and $^3J_{CH}$ values.

In oligosaccharides **11**−**14**, small percentages of *tg* rotamer are observed at the Glc reducing end, regardless of whether O6 is unsubstituted or substituted. A comparison of **12** and **13** shows that O6 substitution increases the *gg*/*gt* ratio.

Most of the compounds exhibit a preference for a gauche orientation between O6H and C5, but as the steric requirements of the substituent at O6 increase, the percentage of trans rotamer increases. This trend is most clearly discerned for **10**, which contains a trityl substituent at O6, although small increases in C6−O6 trans are observed in **11**, **13** and **14** relative to **12**. It is important to appreciate that substitution at O6 eliminates O6H, thereby preventing the measurement of $^3J_{HCOH}$[24b] which can be used to evaluate the C−O torsion. In this situation, knowledge of the relationships between $^2J_{HH}$, $^3J_{HH}$,

**Chart 6**

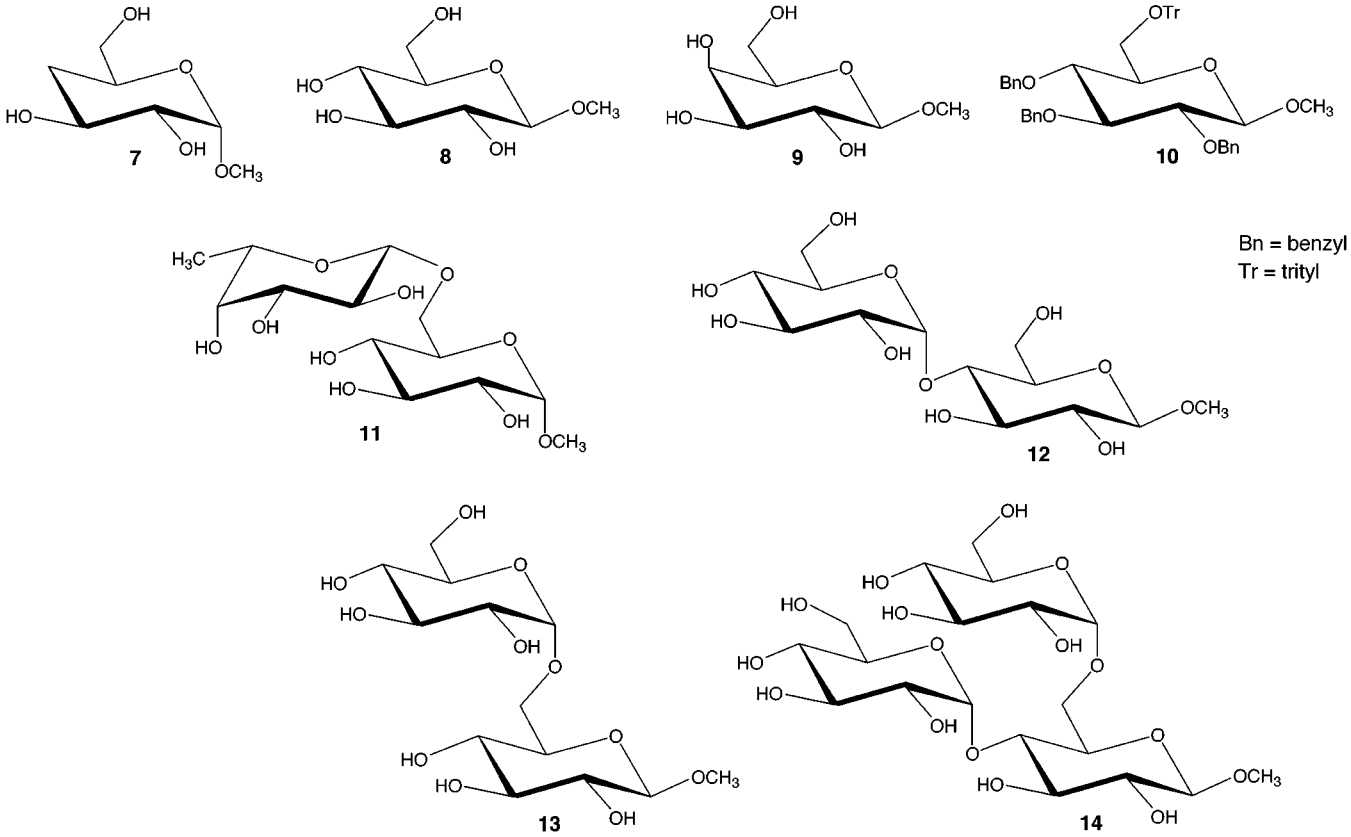


**Table 7. C5−C6 and C6−O6 Rotamer Distributions in 7−14 Calculated from $^2J_{HH}$ and $^3J_{HH}$ Values and the Limiting Coupling Constants[a] in Tables 5 and 6**

| compd[b] | $^3J_{H5,H6R}$ | $^3J_{H5,H6S}$ | $^2J_{H6R,H6S}$ | % *gt* | % *gg* | % *tg* | % C6−O6 trans[c] |
|---|---|---|---|---|---|---|---|
| **7** | 6.3 | 3.2 | −12.0 | 53 | 29 | 18 | 16 |
| **8** | 5.8 | 2.0 | −12.3 | 52 | 41 | 7 | 11 (23)[d] |
| **9** | 8.0 | 4.3 | −11.5 | 67 | 3 | 30 | 28 (27)[d] |
| **10** | 3.6 | 2.0 | −10.0 | 28 | 66 | 6 | 88 |
| **11** | 4.9 | 2.2 | −11.7 | 42 | 51 | 7 | 31 |
| **12**[e] | 5.0 | 2.0 | −12.0 | 45 | 52 | 3 | 22 |
| **13**[e] | 4.0 | 2.0 | −11.4 | 37 | 59 | 4 | 42 |
| **14**[e] | 5.8 | 2.2 | −11.6 | 52 | 41 | 7 | 34 |

[a] From eqs 1−3. [b] Coupling constants for **8** and **10** were taken from ref 29 and for **12**−**14** from ref 30. [c] $\theta = 180°$. [d] Calculated from $^3J_{HCOH}$ values in ref 31 using the Karplus relationship reported in ref 24b. [e] C5−C6 rotamer distributions calculated for the Glc residue at the "reducing" end of the oligosaccharide.

and $\theta$ can be especially useful. Importantly, the calculations yielded positive values for the *tg* rotamer population in all cases. These findings increase the likelihood that the computed rotameric distribution obtained herein is a more accurate representation of behavior in solution. However, these results are still qualitative in that they rely on the accuracy of eqs 1−3, on the assumption that $\omega$ and $\theta$ can be treated independently, and on the assumptions that C5−C6 and C6−O6 bond conformations are each adequately described by a combination of three staggered rotamers undergoing rapid exchange on the NMR time scale. Further improvements are anticipated upon treatment of the remaining *J*-couplings available within exocyclic hydroxymethyl fragments (Chart 3).

## Conclusions

Conformational studies of exocyclic hydroxymethyl groups in saccharides have relied heavily on the use of $^3J_{HH}$ values to estimate rotamer populations in solution, despite the well-known limitations of this experimental approach. While it is self-evident that experimental studies of conformationally flexible molecules or segments of molecules can benefit greatly from the use of multiple and complementary scalar couplings, this approach to studies of $CH_2OH$ conformation has been hampered largely by an incomplete knowledge of these couplings, which include $^2J_{HH}$, $^1J_{CH}$, $^2J_{CH}$, $^3J_{CH}$, $^1J_{CC}$, $^2J_{CC}$, and $^3J_{CC}$. Our aim is to address this deficiency using both experimental and theoretical methods. In the present investigation, we focused exclusively on $^3J_{HH}$, $^2J_{HH}$, and $^1J_{CH}$ values. The strategy was first to obtain experimental data on $^3J_{HH}$ in compounds containing conformationally rigid hydroxymethyl fragments in *gt*, *gg*, and *tg* conformations. These data were then used to test the ability of DFT methods to predict reliable $^3J_{HH}$. We showed through several comparisons of observed and calculated $^3J_{HH}$ that the DFT method yields nearly quantitative results, thus providing a firm basis on which to extend the calculations to $^2J_{HH}$ and $^1J_{CH}$. Several findings emerged from this work, which are summarized as follows.

(A) A new model compound, (2*R*,5*S*)-bis(hydroxymethyl)-1,4-dioxane **1**, was used to establish $^3J_{HH(gauche)}$ and $^3J_{HH(anti)}$ in *gt* rotamers. Similarly, $^3J_{HH}$ values were determined experimentally in fixed *gg* (**2**) and *tg* (**3**) rotamers. These data show that $^3J_{HH(anti)}$ is relatively uniform in magnitude (i.e., substituent effects exert a minor effect on its magnitude), whereas $^3J_{HH(gauche)}$ varies widely because electronegative substituents anti to one of the coupled hydrogens influence the coupling significantly. It is therefore clear that uncertainties in $^3J_{HH(gauche)}$ are likely sources of error in estimates of hydroxymethyl rotamer populations based on $^3J_{HH}$ analysis.

(B) $^3J_{HH}$ values in hydroxymethyl fragments are determined mainly by the C−C torsion angle ($\omega$) and less so by the C−O torsion angle ($\theta$). Calculated $^3J_{H5,H6R}$ and $^3J_{H5,H6S}$ in model compound **5** were used to derive new Karplus equations (eqs 1 and 2) that contain only one geometric variable ($\omega$). This treatment yielded results in excellent agreement with *J*-couplings calculated from a generalized Karplus equation reported previously,[11] thus validating the use of **5** and the $^3J_{HH}$ values calculated therein by the DFT method. In addition, the experimental $^3J_{HH}$ are highly consistent with the DFT-derived $^3J_{HH}$. While these equations represent an improvement in generalized treatments of $^3J_{HH}$ in $CH_2OH$ fragments, it appears that, given the high level of accuracy of the DFT method, the use of *generalized* equations may be less desirable in the future than establishing correlations directly, via calculation, for the specific fragment of interest. The latter approach eliminates complications caused by small substituent effects on the couplings which, in certain situations, may be significant but are averaged out and thus suppressed in the generalized treatments. Thus, for example, it remains unclear whether eqs 1 and 2 can be applied to studies of hydroxymethyl group conformation in nucleosides/tides and their oligomers despite their structural similarities to compounds investigated herein.

(C) $^2J_{HH}$ values in unsubstituted $CH_2OH$ fragments appear to be influenced minimally by the H−C−H bond angle (i.e., this angle appears relatively constant despite changes in $\omega$ and/or $\theta$), but are subject to changes in both $\omega$ and $\theta$. An equation based on the behavior of calculated $^2J_{HH}$ in **5** is proposed in which both $\omega$ and $\theta$ are variables. Since $\omega$ can be estimated from $^3J_{HH}$, this relationship provides a potential means of evaluating C−O torsions that complements other *J*-based methods (i.e., $^3J_{HCOH}$, $^2J_{COH}$, $^3J_{CCOH}$). Importantly, in the absence of an hydroxyl proton on O6 (i.e., when the hydroxyl group is substituted, as in a (1→6)-glycosidic linkage), the latter couplings are unavailable, thus leaving $^2J_{HH}$ as the only remaining $^1H-^1H$ *J*-coupling sensitive to $\theta$. It remains to be established whether *O*-substitution affects the H−C−H bond angle significantly; if so, then this additional factor may need to be considered in structural interpretations of $^2J_{HH}$.

With respect to $^1J_{CH}$ values, previous studies in this laboratory have shown that C−H bond lengths in saccharides are influenced by at least four factors, namely, C−H bond orientation and three types of lone-pair effects (vicinal, 1,3 and 1,4). Consideration of these factors explains reasonably well the calculated behavior of $r_{C6,H6}$ in **5**. This fact alone is reassuring in that it is now possible to anticipate how most C−H, C−C, and C−O bond lengths change in saccharides as a function of conformation, which is prerequisite to understanding other structural, chemical and biochemical phenomena (e.g., isotope effects[32]). The analysis is most satisfying for C−H bonds experiencing only one of these interactions (e.g., the C5−H5 bond in **5**), but even in cases where competing effects are encountered, the observed behavior can be explained qualitatively. While $r_{CH}$ is not expected to be the sole determinant of $^1J_{CH}$, it appears to be a major determinant, such that in most of the cases observed in this study, $r_{CH}$ scales inversely with $^1J_{CH}$. However, although not discussed herein, this inverse relationship is not uniformly obeyed. Preliminary data obtained on **5** by rotating $\theta$ in 30° increments through 360° while holding $\omega$ in staggered rotamers show that,

(25) Ceccarelli, C.; Ruble, J. R.; Jeffrey, G. A. *Acta Crystallogr.* **1980**, *B36*, 861−865.
(26) Nishida, T.; Widmalm, G.; Sandor, P. *Magn. Reson. Chem.* **1996**, *34*, 377−382.
(27) Nishida, Y.; Hori, H.; Ohrui, H.; Meguro, H. *J. Carbohydr. Chem.* **1988**, *7*, 239−250.
(28) Manor, P. C.; Saenger, W.; Davies, D. B.; Jankowski, K.; Rabczenko, A. *Biochim. Biophys. Acta* **1974**, *340*, 472−483.
(29) Rao, V.; Perlin, A. S. *Can. J. Chem.* **1983**, *61*, 2688−2694.
(30) Bock, K.; Pedersen, H. *J. Carbohydr. Chem.* **1984**, *3*, 581−592.
(31) Gillet, B.; Nicole, D.; Delpeuch, J.-J.; Gross, B. *Org. Magn. Reson.* **1981**, *17*, 28−36.
(32) (a) Lewis, B. E.; Schramm, V. L. *J. Am. Chem. Soc.* **2001**, *123*, 1327−1336. (b) Zhu, Y.; Zajicek, J.; Serianni, A. S. *J. Org. Chem.* **2001**, *66*, 6244−6251.

for conformations near (and including) that having the O6−H bond eclipsed with an C6−H6 bond, the C6−H6 bond length decreases but $^1J_{CH}$ also decreases. The cause of this behavior is currently under investigation.

Given the complex interplay of structural factors influencing $^1J_{CH}$, it is not possible to derive an accurate generalized equation relating $^1J_{CH}$ in hydroxymethyl fragments to specific molecular parameters at present. Despite these limitations, however, semiquantitative equations for $^1J_{C6,H6R}$ and $^1J_{C6,H6S}$ have been derived (see Supporting Information) that yield relatively small rms errors (<3 Hz) and relate $^1J_{CH}$ to both $\omega$ and $\theta$.

Applications of the *J*-coupling correlations were made using a three-state staggered rotamer model,[24a] but other treatments of *J*-couplings and NMR observables have been described. For example, Dzakula *et al.*[33] have proposed the CUPID method of data analysis that does not involve assumptions about fixed staggered rotamers, yielding a continuous rotamer population distribution. In a similar vein, Poppe[34] reported the use of the maximum entropy method to derive rotameric distributions from experimental constraints. The success of these methods depends on the availability of multiple experimental observables; for CUPID, six conformationally sensitive parameters are required. The development of *J*-couplings beyond $^3J_{HH}$ (see Chart 3) to probe $CH_2OH$ conformation may promote the use of these more sophisticated treatments, which presumably lead to more accurate representations of C5−C6 bond conformation in solution.

The present work again demonstrates the reliability of the DFT method as a tool to predict scalar couplings involving $^1H$ and $^{13}C$ nearly quantitatively, and establishes new formulas for the interpretation of $^2J_{HH}$ and $^3J_{HH}$ in the hydroxymethyl groups of saccharides. We will report shortly related studies of $^2J_{CH}$, $^3J_{CH}$, $^2J_{CC}$, and $^3J_{CC}$ as complementary conformational constraints.

**Acknowledgment.** This work was supported by a postdoctoral fellowship from the Knut och Alice Wallenberg stiftelse (Stockholm, Sweden) to R.S., a grant from the Swedish Research Council to G.W., and grants from Omicron Biochemicals, Inc. of South Bend, IN and from the Office of Basic Energy Sciences of the United States Department of Energy. This is Document No. NDRL-4315 from the Notre Dame Radiation Laboratory.

**Supporting Information Available:** Discussion of equations relating $^1J_{CH}$ in **5** to $\omega$ and $\theta$, and two figures showing hypersurfaces relating $^1J_{C6,H6R}$ and $^1J_{C6,H6S}$ to these torsion angles. This material is available free of charge via the Internet at http://pubs.acs.org.

JO010985I

(33) (a) Dzakula, Z.; Westler, W. M.; Edison, A. S.; Markley, J. L. *J. Am. Chem. Soc.* **1992**, *114*, 6195. (b) Dzakula, Z.; Edison, A. S.; Westler, W. M.; Markley, J. L. *J. Am. Chem. Soc.* **1992**, *114*, 6200.

(34) Poppe, L. *J. Am. Chem. Soc.* **1993**, *115*, 8421.